((please add journal code and manuscript number, e.g., DOI: 10.1002/ppap.201100001))
Article type: Full paper

Plasma-catalytic reforming of biogas over supported Ni catalysts in a dielectric barrier discharge reactor: Effect of catalyst supports

Danhua Mei, Bryony Ashford, Ya-Ling He, Xin Tu*

———

D. H. Mei, B. Ashford, Dr. X. Tu
Department of Electrical Engineering and Electronics, University of Liverpool, Brownlow Hill, Liverpool, L69 3GJ, UK
E-mail: xin.tu@liverpool.ac.uk

D. H. Mei, Prof. Y.-L. He
Key Laboratory of Thermo-Fluid Science and Engineering, Ministry of Education, School of Energy and Power Engineering, Xi'an Jiaotong University, Xi'an 710049, China

———

Corresponding author

Dr. Xin Tu

Department of Electrical Engineering and Electronics

University of Liverpool

Liverpool L69 3GJ

UK

E-mail: xin.tu@liverpool.ac.uk

Abstract

In this study, plasma-catalytic reforming of simulated biogas for the production of value-added fuels and chemicals (e.g. H_2) has been carried out in a coaxial dielectric barrier discharge (DBD) plasma reactor. The influence of four Ni catalysts (Ni/γ-Al_2O_3, Ni/MgO, Ni/SiO_2 and Ni/TiO_2) on the plasma-catalytic biogas reforming has been investigated in terms of the conversion of reactants, the yield and selectivity of target products, the carbon deposition on the catalysts and the energy efficiency of the plasma-catalytic process. The use of plasma combined with these Ni catalysts enhanced the performance of the biogas reforming. A maximum CO_2 conversion of 26.2% and CH_4 conversion of 44.1% were achieved when using the Ni/γ-Al_2O_3 catalyst at a specific energy density (SED) of 72 kJ l^{-1}. Compared to other Ni catalysts, placing the Ni/γ-Al_2O_3 catalyst in the DBD produced more syngas and C_3-C_4 hydrocarbons, but less C_2H_6. The lowest energy cost (EC) for biogas conversion and syngas production, as well as the highest energy efficiency and fuel production efficiency (FPE), were achieved when using the Ni/γ-Al_2O_3 catalyst in the plasma process. The Ni/γ-Al_2O_3 catalyst also showed the lowest surface carbon deposition of 3.8%, after catalysing the plasma biogas reforming process for 150 min at a SED of 60 kJ l^{-1}. Compared to other Ni catalysts, the enhanced performance of the Ni/γ-Al_2O_3 catalyst can be attributed to its higher specific surface area, higher reducibility and more, stronger basic sites on the catalyst surface.

Graphic for the abstract

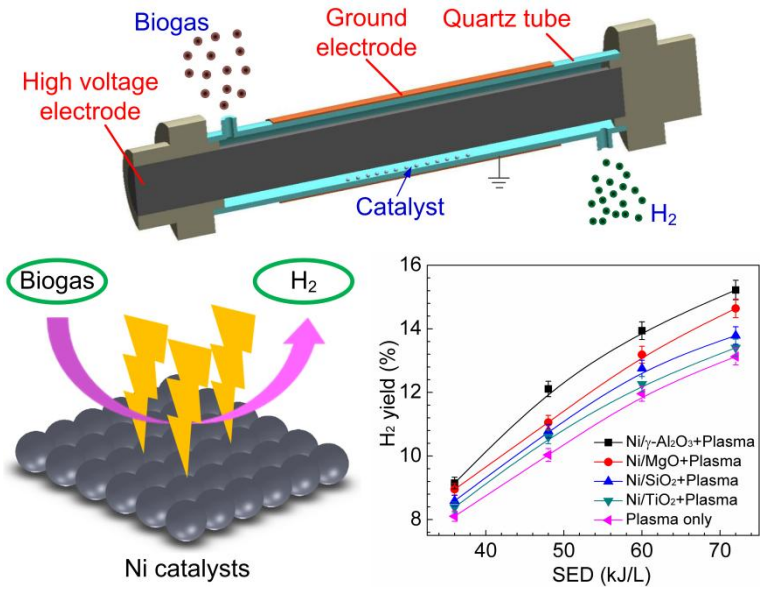

1. Introduction

Biogas is considered a promising renewable energy source that could respond to the vital societal need for an increase in the sustainability of energy production which is required to combat climate change. Biogas mainly consists of methane (50-75%) and carbon dioxide (25-50%), and can be produced from the anaerobic digestion of biomass, landfill and wastewater treatment. The United Kingdom is currently the second largest biogas producer in Europe.[1] Biogas can be used for the generation of electricity and heating but suffers from high emissions and a low heating value due to its high CO_2 content. Biogas upgrading is a process which removes CO_2, generating a CH_4-rich biogas that can be used as a substitute for natural gas in a wide range of applications. However, separating CO_2 from biogas is an energy intensive and costly process. Catalytic reforming of biogas without prior CO_2 separation (also called dry reforming of methane) represents an effective and sustainable route to produce syngas (a mixture of CO and H_2), which is an important chemical feedstock for the production of liquid fuels and can also be used in fuel cells.

$$CH_4 + CO_2 \rightarrow 2H_2 + 2CO \qquad \Delta H = 247 \text{kJ mol}^{-1} \tag{1}$$

However, one of the major challenges in the conventional catalytic biogas reforming process is the high energy cost as elevated process temperatures (>700 ^oC) are required to obtain reasonable conversions of biogas and yields of syngas in this highly endothermic reaction. In addition, rapid deactivation of reforming catalysts due to carbon deposition on the catalyst surface limits the use of this process on a commercial scale.

The non-thermal plasma process offers an attractive alternative to the conventional catalytic route for biogas reforming at low temperatures. In non-thermal plasmas, there is a significant difference in the temperature between the electrons and heavy particles. The overall gas kinetic temperature of a plasma can be as low as room temperature, while the produced electrons are highly energetic (e.g., 1-10 eV) and can break most chemical bonds within molecules (e.g. CH_4) as well as producing a variety of chemically reactive species: free

radicals, excited atoms, ions and molecules for the initiation and propagation of chemical reactions.[2, 3] The non-equilibrium character of such plasmas could overcome thermodynamic barriers in chemical reactions and enable thermodynamically unfavourable reactions (e.g. biogas reforming) to occur under ambient conditions. High reaction rate and fast attainment of steady state in plasma processes allows rapid start-up and shutdown of the process compared to other thermal processes, which significantly reduces the energy cost and offers a promising route for industrial applications.

The combination of non-thermal plasma and catalyst, known as plasma-catalysis, has great potential to generate a low temperature synergistic effect as a result of the interactions between the plasma and catalyst. It can also lower the activation energy of the catalyst, as well as improve its activity and stability. This can result in the enhancement of reactant conversion, selectivity and yield of end-products and the energy efficiency of the process.[4, 5] Previous works have shown that catalysts can be easily integrated with a dielectric barrier discharge (DBD) system for gas conversion and fuel production.[6-8] Moreover, DBD has been proven to be a successful technology for ozone generation and gas clean-up on an industrial scale.[9, 10]

Zeolites and metal catalysts have been used before in plasma-catalytic dry reforming of CH_4, such as Zeolite 3A,[11] NaX and NaY,[12, 13] Ni/γ-Al_2O_3,[8, 14-17] Ag/Al_2O_3,[18] Pd/Al_2O_3,[18, 19] Cu-Ni/Al_2O_3,[20] Cu/Al_2O_3,[17, 19] Co/γ-Al_2O_3,[17] Mn/γ-Al_2O_3,[17] Fe/Al_2O_3,[21] La_2O_3/γ-Al_2O_3,[22] $LaNiO_3$,[23] and $LaNiO_3$@SiO_2.[24, 25] Ni/γ-Al_2O_3 has been the most commonly used catalyst in the plasma-catalytic reforming process, while γ-Al_2O_3 has been the most frequently used support for the preparation of these metal catalysts. Clearly, compared to thermal catalytic dry reforming of methane, a very limited number of catalysts have been evaluated for use in the plasma-catalytic methane reforming reaction. Furthermore, the synergistic effect from the combination of plasma and these catalysts has not been fully investigated and understood. Moreover, very few works have been devoted to the modification of Ni catalysts

(e.g. using different supports or promoters) to further enhance their catalytic activity in the plasma-catalytic dry reforming process. For instance, the catalyst support has been reported to play a key role in determining the surface area, acid-base properties, pore properties and metal dispersion of a catalyst. These catalyst properties consequently affect the activity and stability of the catalyst in methane reforming reactions.[26] Different supports (e.g. γ-Al_2O_3, MgO, SiO_2, TiO_2, etc.) have been widely used in thermal-catalytic dry reforming of CH_4,[26, 27] however to the best of our knowledge, far less research has been conducted to understand the effect of different supported Ni catalysts on the plasma reforming of biogas. The fundamental understanding of the catalyst properties in the plasma-catalytic reforming process is still very limited. Therefore, it is important to get new insights into the roles of different catalyst supports in the plasma biogas reforming and to establish a relationship between the plasma reforming performance and catalyst properties.

In this work, plasma-catalytic reforming of biogas over four Ni catalysts supported on different compounds (γ-Al_2O_3, MgO, SiO_2 and TiO_2) has been investigated in a coaxial DBD reactor. The effect of these catalysts on the plasma biogas reforming as a function of specific energy density (SED) is evaluated in terms of the conversion of reactant gases, the yield and selectivity of gas products, the carbon deposition on the spent catalysts and the energy efficiency of the plasma-catalytic reforming process. Different catalyst characterization including N_2 adsorption-desorption, X-ray diffraction (XRD), temperature-programmed desorption of CO_2 (CO_2-TPD), temperature-programmed reduction by H_2 (H_2-TPR) and thermo-gravimetric analysis (TGA), has been used to understand the effect of catalyst properties on the plasma reforming of biogas.

2. Experimental

2.1 Catalyst preparation and characterisation

The Ni catalysts on different supports (γ-Al_2O_3, MgO, SiO_2 and TiO_2, Aladdin® China) with a Ni loading of 10 wt.% were prepared by incipient wetness impregnation using $Ni(NO_3)_2{\cdot}6H_2O$ as the metal precursor. The appropriate weight of support (1 mm diameter beads) was added to the metal precursor solution and impregnated for 12 hours. After that the solution was evaporated at 80 ^oC for 4 h and dried at 110 ^oC overnight, followed by calcination in air at 400 ^oC for 4 h.

To understand the surface properties of the catalysts, N_2 adsorption-desorption isotherms were carried out at 77 K to measure the pore size and specific surface area of the catalysts using a surface area analyzer (Quantachrome NOVA 4200e). Before each measurement, the samples were outgassed at 300 ^oC for 2 h under vacuum to remove moisture and other adsorbed gases. XRD patterns of the catalyst samples were recorded by an X-ray diffractometer (Rigaku, SmartLab) equipped with Cu-Kα radiation (40 kV tube voltage and 40 mA tube current) in the scanning range 2θ between 10^o and 80^o. The amount of basic sites on the catalysts was determined by temperature-programmed desorption of CO_2 using a fully automated chemisorption analyzer (AutoChem II 2920). The CO_2 adsorption was carried out at room temperature for 30 min using a CO_2/He gas mixture (V/V, 10/90) with a flow rate of 50 ml min^{-1}. Afterwards, the TPD-CO_2 signal was recorded with the temperature increasing from 40 ^oC to 700 ^oC at a heating rate of 10 ^oC min^{-1}. The reducibility of the catalysts was evaluated by H_2-TPR using the same automated chemisorption analyzer. Prior to each run, the 90 mg catalyst sample was pre-treated at 200 ^oC for 40 min under Ar flow to remove physically adsorbed and/or weakly bound species. After cooling to room temperature, the sample was heated from 20 ^oC to 800 ^oC with a heating rate of 10 ^oC min^{-1} using a CO_2/Ar gas mixture (V/V, 10/90) with a flow rate of 30 ml min^{-1}. The coke deposition on the spent catalysts was analysed by the thermo-gravimetric analysis in air atmosphere using a TA

Instruments SDT-Q600. Each spent catalyst (20 mg) was heated from 30 ℃ to 800 ^{o}C at a heating rate of 10 ^{o}C min^{-1} with an air flow of 30 ml min^{-1}.

2.2 Experimental setup

The experiments were carried out in a coaxial DBD reactor, as shown in Figure 1. A 10 cm long stainless steel mesh was wrapped around a quartz tube with an external diameter of 25 mm and an inner diameter of 22 mm. A stainless steel rod with an outer diameter of 17 mm was placed in the centre of the quartz tube and acted as an inner electrode. As a result, the discharge gap was 2.5 mm with a discharge volume of 15.3 ml. The inner electrode was connected to a high voltage output and the outer electrode was grounded via an external capacitor C_{ext} (0.47 μF). CO_2 and CH_4 gas mixture with a molar ratio of 1:1 was used as the simulated biogas. The feed flow rate of the simulated biogas was fixed at 50 ml min^{-1}. 0.5 g of Ni catalyst pellets (1 mm in diameter) were placed along the bottom of the DBD reactor in the discharge region, partially filling the discharge gap. This partial packing method has been shown to enhance plasma-catalyst interactions and plasma chemical reactions in previous studies.[6, 8] Prior to the plasma-catalytic biogas reforming reaction, the supported Ni catalyst pellets were in-situ reduced in an Ar-H_2 discharge for 30 min in the same DBD reactor. The discharge power was 50 W, with a total flow rate of 50 ml min^{-1} (20 vol.% H_2). The plasma reforming reaction was carried out after the reduced catalyst had cooled down to room temperature in the Ar atmosphere.

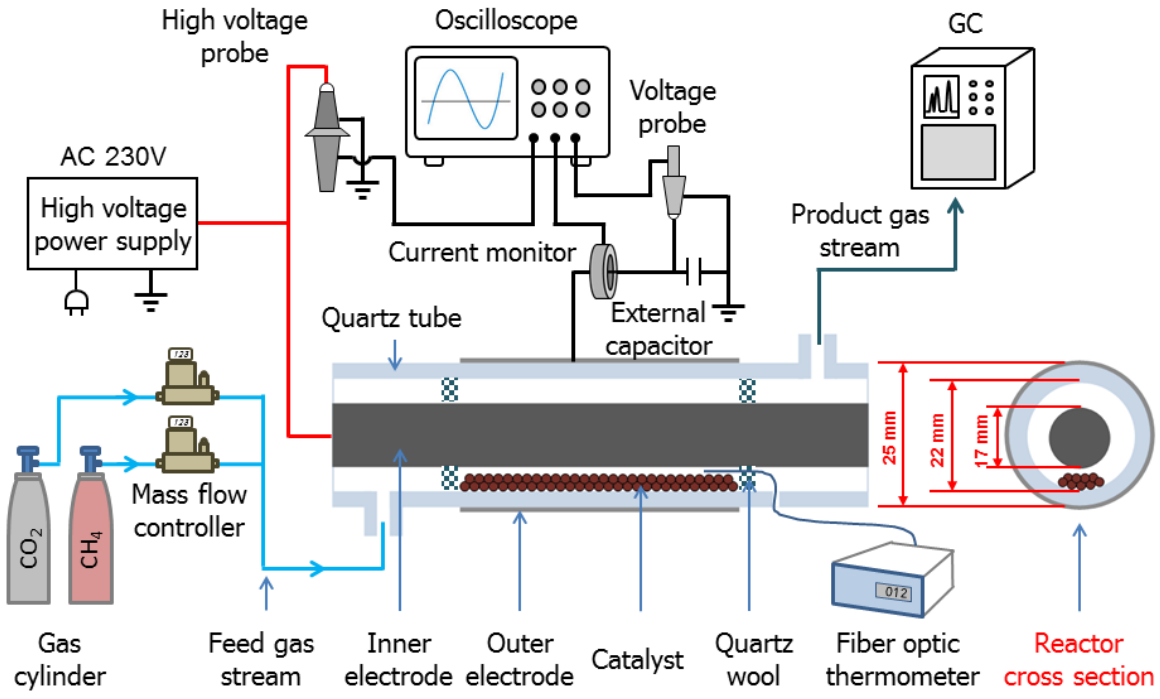

Figure 1. Schematic of the experimental setup.

The DBD reactor was connected to an AC high voltage power supply with a maximum peak voltage of 30 kV and a frequency range of 5-20 kHz. The applied voltage (U_a) was measured by a high voltage probe (Testec, HVP-15HF), whilst the current (I_t) was recorded by a current monitor (Bergoz CT-E0.5). The voltage (U_c) on the external capacitor was measured to obtain the charge generated in the discharge. All the electrical signals were sampled by a four-channel digital oscilloscope (TDS2014). The discharge power was obtained by the area calculation of the *Q-U* Lissajous figure. A homemade online power measurement system was used to monitor and control the discharge power in real time.

The specific energy density of the plasma reactor can be determined by

$$\mathrm{SED}\left(\mathrm{kJ\,L^{-1}}\right)=\frac{60\times P\left(\mathrm{W}\right)}{q\left(\mathrm{ml\,min^{-1}}\right)} \tag{2}$$

where P and q are the discharge power and total feed flow rate, respectively.

The gas temperature in the DBD reactor was measured by a fiber optical temperature probe (Omega, FOB102) inserted into the discharge area through a hole in the quartz tube. The feed

and product gases were analyzed by a two-channel gas chromatograph (Shimadzu GC-2014) equipped with a flame ionization detector (FID) and a thermal conductivity detector (TCD). The GC was calibrated for a wide range of concentrations for each gaseous component using standard gas mixtures (Air Liquid) and other calibrated gas mixtures. An hour after the system had reached a steady state, gas products were sampled and measured three times. CO_2 conversion, CH_4 conversion and total carbon conversion are defined as

$$C_{\mathrm{CO_2}}(\%) = \frac{\mathrm{CO_2\ converted}\ \left(\mathrm{mol\ s^{-1}}\right)}{\mathrm{CO_2\ input}\ \left(\mathrm{mol\ s^{-1}}\right)} \times 100 \tag{3}$$

$$C_{\mathrm{CH_4}}(\%) = \frac{\mathrm{CH_4\ converted}\ \left(\mathrm{mol\ s^{-1}}\right)}{\mathrm{CH_4\ input}\ \left(\mathrm{mol\ s^{-1}}\right)} \times 100 \tag{4}$$

$$C_{\mathrm{TC}}(\%) = x_{\mathrm{CO_2}} \times C_{\mathrm{CO_2}} + x_{\mathrm{CH_4}} \times C_{\mathrm{CH_4}} \tag{5}$$

where $x_{\mathrm{CO_2}}$ and $x_{\mathrm{CH_4}}$ are the percentage concentration of CO_2 and CH_4 in the gas mixture, respectively.

The selectivities (S) and yields (Y) of the main reforming products are calculated by

$$S_{\mathrm{H_2}}(\%) = \frac{\mathrm{H_2\ produced}\ \left(\mathrm{mol\ s^{-1}}\right)}{2 \times \mathrm{CH_4\ converted}\ \left(\mathrm{mol\ s^{-1}}\right)} \times 100 \tag{6}$$

$$S_{\mathrm{CO}}(\%) = \frac{\mathrm{CO\ produced}\ \left(\mathrm{mol\ s^{-1}}\right)}{\mathrm{CH_4\ converted}\ \left(\mathrm{mol\ s^{-1}}\right) + \mathrm{CO_2\ converted}\ \left(\mathrm{mol\ s^{-1}}\right)} \times 100 \tag{7}$$

$$S_{\mathrm{C_xH_y}}(\%) = \frac{x \times \mathrm{C_xH_y\ produced}\ \left(\mathrm{mol\ s^{-1}}\right)}{\mathrm{CH_4\ converted}\ \left(\mathrm{mol\ s^{-1}}\right) + \mathrm{CO_2\ converted}\ \left(\mathrm{mol\ s^{-1}}\right)} \times 100 \tag{8}$$

$$Y_{\mathrm{H_2}}(\%) = \frac{\mathrm{H_2\ produced}\ \left(\mathrm{mol\ s^{-1}}\right)}{2 \times \mathrm{CH_4\ input}\ \left(\mathrm{mol\ s^{-1}}\right)} \times 100 \tag{9}$$

$$Y_{\mathrm{CO}}(\%) = \frac{\mathrm{CO\ produced}\ \left(\mathrm{mol\ s^{-1}}\right)}{\mathrm{CH_4\ input}\ \left(\mathrm{mol\ s^{-1}}\right) + \mathrm{CO_2\ input}\ \left(\mathrm{mol\ s^{-1}}\right)} \times 100 \tag{10}$$

The carbon balance (B) of the plasma biogas reforming process is determined as follows:

$$B_{\text{Carbon}}(\%) = \frac{[\text{CH}_4 + \text{CO}_2]\text{unconverted}\left(\text{mol s}^{-1}\right) + [\text{CO} + 2\times\text{C}_2 + 3\times\text{C}_3 + 4\times\text{C}_4]\text{produced}\left(\text{mol s}^{-1}\right)}{[\text{CH}_4 + \text{CO}_2]\text{input}\left(\text{mol s}^{-1}\right)} \times 100 \quad (11)$$

To evaluate the energy efficiency of the plasma biogas reforming process, the energy cost (EC) for CO_2 conversion (EC_{CO_2}), CH_4 conversion (EC_{CH_4}) and total carbon conversion (EC_{TC}) are defined as follows:

$$\text{EC}_{\text{CO}_2}\left(\text{MJ mol}^{-1}\right) = \frac{\text{Discharge power}(\text{kW})}{1000\times\text{CO}_2\text{ input}\left(\text{mol s}^{-1}\right)\times C_{\text{CO}_2}(\%)} \quad (12)$$

$$\text{EC}_{\text{CH}_4}\left(\text{MJ mol}^{-1}\right) = \frac{\text{Discharge power}(\text{kW})}{1000\times\text{CH}_4\text{ input}\left(\text{mol s}^{-1}\right)\times C_{\text{CH}_4}(\%)} \quad (13)$$

$$\text{EC}_{\text{TC}}\left(\text{MJ mol}^{-1}\right) = \frac{\text{Discharge power}(\text{kW})}{1000\times\left(\text{CH}_4\text{ input}\left(\text{mol s}^{-1}\right) + \text{CO}_2\text{ input}\left(\text{mol s}^{-1}\right)\right)\times C_{\text{TC}}(\%)} \quad (14)$$

The energy cost for the production of H_2 (EC_{H_2}) and syngas (EC_{Syngas}), the energy efficiency (EE) and the fuel production efficiency (FPE) are determined by:

$$\text{EC}_{\text{H}_2}\left(\text{MJ mol}^{-1}\right) = \frac{\text{Discharge power}(\text{kW})}{1000\times\text{H}_2\text{ produced}\left(\text{mol s}^{-1}\right)} \quad (15)$$

$$\text{EC}_{\text{Syngas}}\left(\text{MJ mol}^{-1}\right) = \frac{\text{Discharge power}(\text{kW})}{1000\times\left(\text{H}_2\text{ produced}\left(\text{mol s}^{-1}\right) + \text{CO produced}\left(\text{mol s}^{-1}\right)\right)} \quad (16)$$

$$\text{EE}\left(\text{mmol kJ}^{-1}\right) = \frac{\text{CH}_4\text{ converted}\left(\text{mol s}^{-1}\right) + \text{CO}_2\text{ converted}\left(\text{mol s}^{-1}\right)}{\text{Power}(\text{W})} \quad (17)$$

$$\text{FPE}(\%) = \frac{\sum\text{fuel produced}\left(\text{mol s}^{-1}\right)\times\text{LHV}\left(\text{kJ mol}^{-1}\right)}{\text{CH}_4\text{ converted}\left(\text{mol s}^{-1}\right)\times\text{LHV of CH}_4\left(\text{kJ mol}^{-1}\right) + \text{Discharge power}(\text{kW})} \times 100 \quad (18)$$

where LHV is the low heating value of the fuel, as shown in Table 1.

Table 1. LHV of different fuels (kJ mol^{-1}, 25 ^oC). [28]

Fuel	CH_4	C_2H_6	C_2H_4	C_2H_2	C_3H_8	C_4H_{10}	CO	H_2

LHV	802.3	1437.2	1323.8	1256.2	2044.2	2659.3	283.2	241.8

3. Results and discussion

3.1 Catalyst characterization

3.1.1 Surface structure of the catalysts

Table 2 lists the physicochemical properties of the fresh Ni catalysts. Clearly, the Ni/γ-Al_2O_3 catalyst shows the highest specific surface area at 268.0 m^2 g^{-1} and largest pore volume at 0.39 cm^3 g^{-1}, followed by the Ni/MgO, Ni/SiO_2 and Ni/TiO_2 catalysts. The specific surface area of the Ni/γ-Al_2O_3 catalyst is more than twice that of the Ni/TiO_2 catalyst, whilst the Ni/TiO_2 catalyst has the largest pore diameter at more than double the value of the Ni/γ-Al_2O_3 catalyst.

Table 2. Physicochemical properties of the Ni catalysts

Sample	S_{BET} (m^2 g^{-1})	Pore volume (cm^3 g^{-1})	Average pore diameter (nm)
Ni/γ-Al_2O_3	268.0	0.39	3.80
Ni/MgO	193.8	0.36	4.25
Ni/SiO_2	166.4	0.33	6.73
Ni/TiO_2	103.6	0.26	7.84

Figure 2 shows the XRD patterns of the fresh Ni catalysts. The NiO peaks are clearly shown in the XRD spectra of the Ni/γ-Al_2O_3, Ni/SiO_2 and Ni/TiO_2 catalysts. For the Ni/MgO catalyst, it is well known that both NiO and MgO have a NaCl-lattice structure. It is difficult to distinguish NiO peaks from MgO peaks due to similar dimensions of their respective unit cells.[29] However, for the Ni catalysts calcined at 400 ^oC, the NiO species could only partially

be incorporated into the lattice of the MgO support, whilst the remaining NiO exists in the form of free NiO on the catalyst surface due to weak interactions between MgO and the Ni precursor.[30] Previous works showed that NiO on the catalyst surface can be reduced to Ni by low temperature Ar-H_2 plasmas.[17, 31] Compared to the Ni/MgO, Ni/SiO_2 and Ni/TiO_2 catalysts, the NiO peaks in the XRD pattern of the Ni/γ-Al_2O_3 catalyst are weaker and broader, indicating that NiO might be dispersed to a greater extent on the surface of the Ni/γ-Al_2O_3 catalyst.

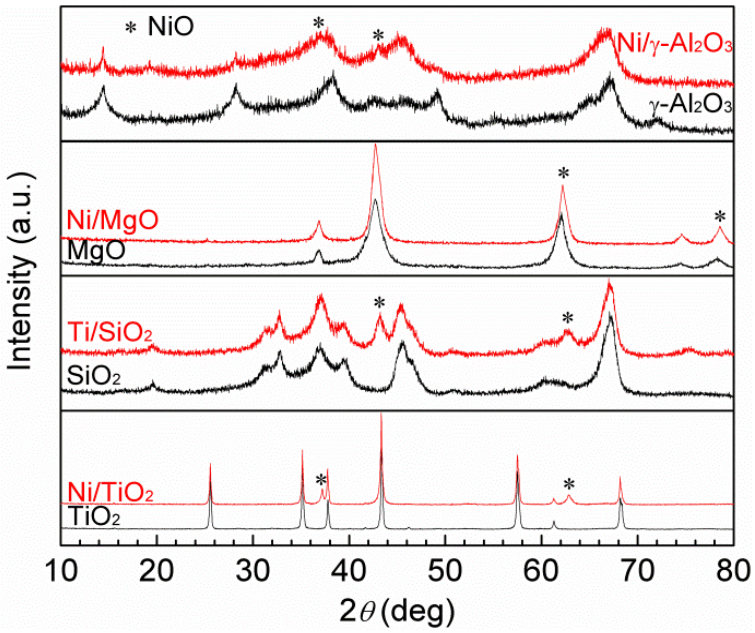

Figure 2. XRD patterns of supports and fresh catalysts.

3.1.2 CO_2-TPD

It has been reported that CO_2 adsorbed on weak basic sites of a catalyst is desorbed at low temperatures, while CO_2 adsorbed on strong basic sites is desorbed at high temperatures.[32] Generally, the weak, intermediate, strong and very strong basic sites on the catalyst surface correspond to the peaks within the temperature ranges of 20-150 ^oC, 150-300 ^oC, 300-450 ^oC and > 450 ^oC in a CO_2-TPD profile, respectively.[32] The number of basic sites on the catalyst surface can be estimated from the area under their CO_2-TPD curves.[32] Figure 3 shows the

CO_2-TPD patterns of the fresh Ni catalysts. Clearly, the Ni/γ-Al_2O_3, Ni/MgO and Ni/SiO_2 catalysts show three CO_2 desorption peaks: the first two peaks are centred at 50-100 ^oC and 120-200 ^oC, indicating the formation of weak basic sites on the catalyst surface, whilst the third one at 300 - 500 ^oC can be attributed to the generation of strong basic sites. The peak area associated to the strong basic sites on the Ni/γ-Al_2O_3 catalyst is much larger than that of the Ni/MgO and Ni/SiO_2 catalysts, which suggests that more strong basic sites are formed on the surface of the Ni/γ-Al_2O_3 catalyst. In contrast, the Ni/TiO_2 catalyst only shows a weak CO_2 desorption peak at 50-100 ^oC. These results indicate that the Ni/γ-Al_2O_3 catalyst has the highest number of strong basic sites, followed by the Ni/MgO, Ni/SiO_2 and Ni/TiO_2 catalysts. CO_2 chemisorption and activation, which are beneficial for improving the conversions of CO_2 and CH_4, occur to a greater extent when the catalyst contains strong basic sites. In addition, adsorbed CO_2 on the catalyst surface may eliminate carbon deposition as the presence of surface oxygen from acidic CO_2 can result in carbon gasification;[33, 34] thus, the Ni/γ-Al_2O_3 catalyst is expected to have a higher catalytic performance and coke resistance in comparison to the other catalysts.

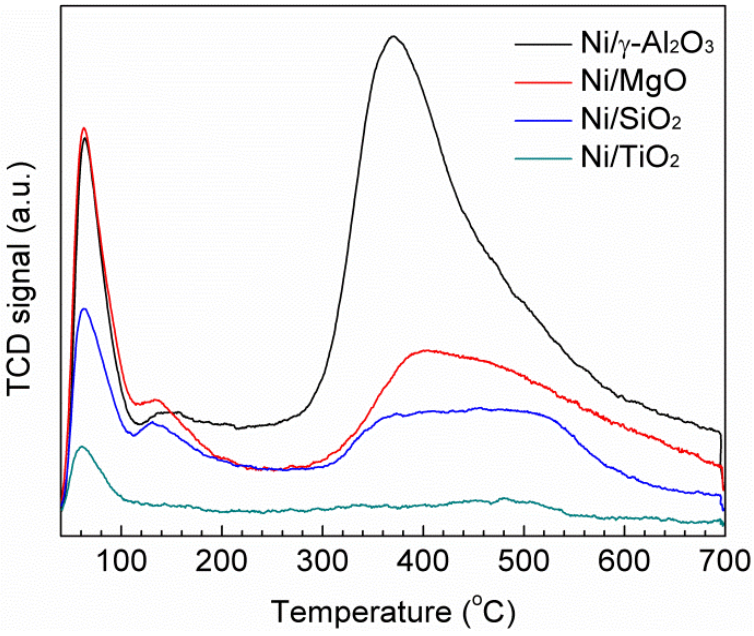

Figure 3. CO_2-TPD patterns of the Ni catalysts.

3.1.3 H_2-TPR

Figure 4 shows the H_2-TPR profiles of the Ni catalysts. The Ni/γ-Al_2O_3 catalyst exhibits two major peaks: the first peak at 380 ^oC is related to the reduction of bulk NiO, while the second peak at 570 ^oC can be ascribed to the reduction of NiO due to the medium-strength interaction with the γ-Al_2O_3 support. $NiAl_2O_4$ is generally formed in high temperature (> 700 ^oC) calcination due to strong interactions between Al_2O_3 support and Ni precursor. In Figure 4, no peak is associated with the high temperature reduction (> 700 ^oC) of $NiAl_2O_4$ due to the low temperature calcination of these catalysts at 400 ^oC. These findings suggest that NiO could be dominant on the γ-Al_2O_3 support. Similarly, two distinct peaks (440 ^oC and 680 ^oC) in the H_2-TPR profile of the Ni/MgO catalyst can also be associated to the reduction of NiO. The Ni/SiO_2 catalyst shows only one low temperature reduction peak at around 375 ^oC, while the TPR profile of the Ni/TiO_2 catalyst exhibits a broad peak between 265-600 ^oC. Cleary, the H_2-TPR profiles of all the catalysts show low temperature peaks related to the reduction of NiO due to weak and/or intermediate interactions between support and Ni precursor. The reducibility of the supported Ni catalysts follows the order of Ni/γ-Al_2O_3, Ni/MgO, Ni/SiO_2 and Ni/TiO_2. It was reported that the peak area in the H_2-TPR profiles is proportional to the reduced amount of Ni species.[35] Therefore, the Ni/γ-Al_2O_3 catalyst has the highest amount of reduced Ni, followed by the Ni/MgO, Ni/SiO_2 and Ni/TiO_2 catalysts.

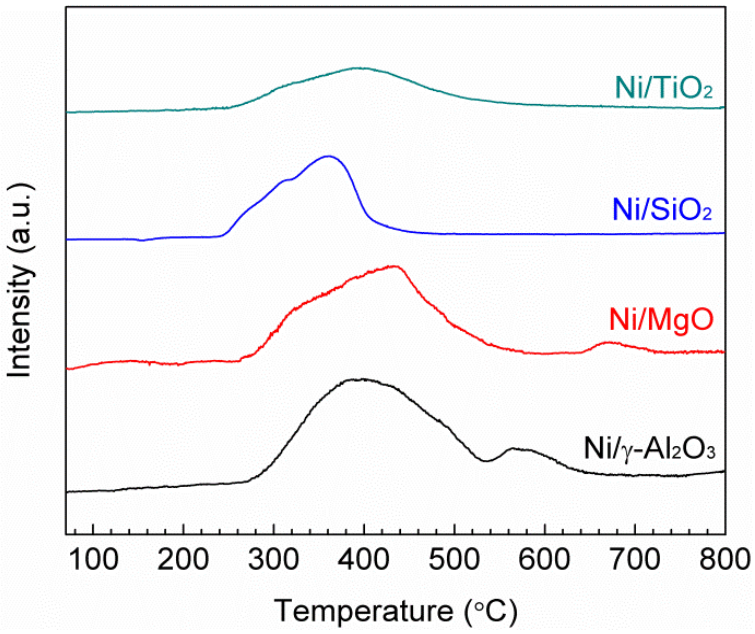

Figure 4. H_2-TPR patterns of the Ni catalysts

3.2 Plasma-catalytic reforming of biogas

3.2.1 Biogas conversion

The effect of Ni catalysts with different supports on the conversions of CO_2 and CH_4 as a function of SED is shown in Figure 5. Both CO_2 and CH_4 conversions are increased by increasing the SED, regardless of the catalyst used. In this study, the SED can be controlled by changing the applied voltage at a fixed frequency and feed flow rate. Increasing the SED by only raising the applied voltage increases the number of microdischarges and current intensity in the DBD reactor,[36] which indicates that more reaction channels and electrons could be formed to activate reactants in the plasma reaction;[37] both of these factors contribute to the enhancement of the conversion of CO_2 and CH_4.

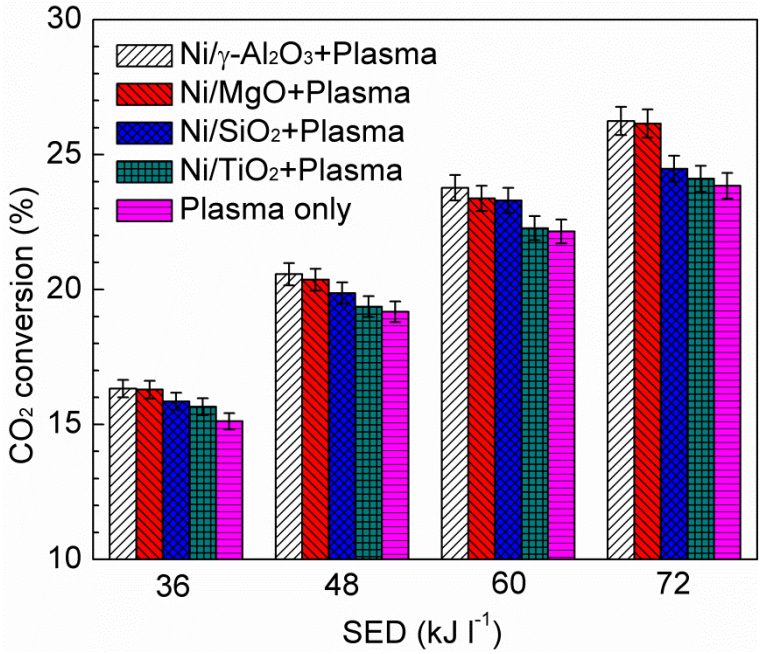

(a)

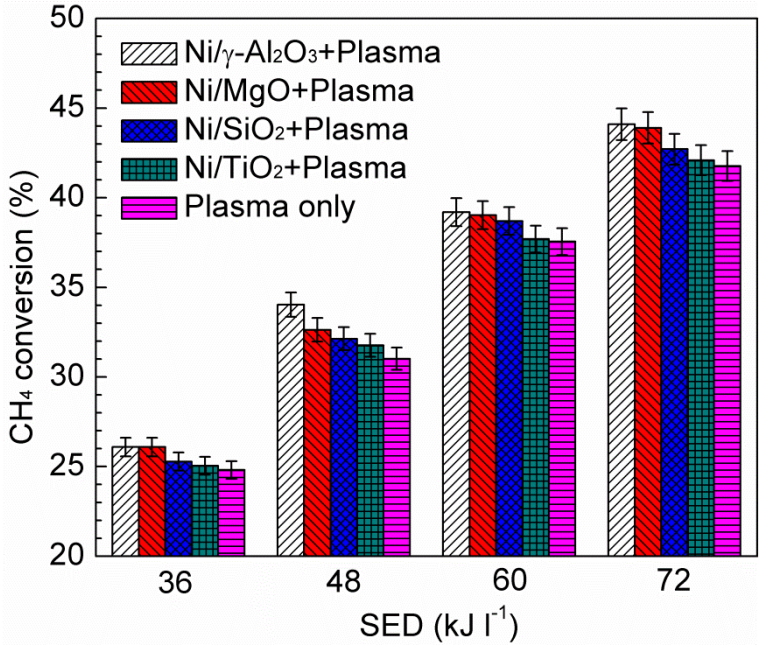

(b)

Figure 5. Effect of different Ni catalysts on (a) CO_2 conversion and (b) CH_4 conversion as a function of SED (total feed flow rate: 50 ml min^{-1}; CO_2/CH_4 molar ratio: 1:1).

In the plasma dry reforming of undiluted CH_4 and CO_2 in a DBD, the initial reactions for the conversion of CO_2 and CH_4 are mainly driven by electron-impact dissociation of CO_2 and

CH_4 (Equation 19 to 22). More reaction pathways exist for CH_4 conversion to generate CH_3, CH_2 and CH (Equation 20 to 22), followed by radical recombination reactions to form higher hydrocarbons or further electron-impact dissociation of radicals.

$$CO_2 + e \rightarrow CO + O + e \quad (19)$$

$$CH_4 + e \rightarrow CH_3 + H + e \quad (20)$$

$$CH_4 + e \rightarrow CH_2 + H_2 + e \quad (21)$$

$$CH_4 + e \rightarrow CH + H + H_2 + e \quad (22)$$

CO_2 and CH_4 can promote the conversion of each other when they are co-fed to a plasma reactor, compared to the conversion of pure CO_2 or CH_4.[38] Atomic oxygen species from the dissociation of CO_2 can also break the C-H bond in CH_4, as shown in Equation 23, while hydrogen atoms from CH_4 dissociation can facilitate the conversion of CO_2 (Equation 24). However, the rate coefficient of the reaction (Equation 23) is several orders of magnitude higher than that of the reaction (Equation 24) in the temperature range of 300-2500 K.[38] This may be one of the reasons for the less pronounced CO_2 conversion compared to that of CH_4 in the plasma reforming of biogas.

$$CH_4 + O \rightarrow CH_3 + OH,\ k = 8.75\times10^{-12}\times(T/298)^{1.5}\exp(-4330/T) \quad (23)$$

$$CO_2 + H \rightarrow OH + CO,\ k = 2.5\times10^{-10}\exp(-13300/T) \quad (24)$$

In addition, recent simulation showed that the following reaction plays a dominant role in producing CO_2 in the plasma dry reforming reaction in a DBD reactor, leading to a lower CO_2 conversion compared to the conversion of CH_4.[39]

$$CO_2^+ + CH_4 \rightarrow CH_4^+ + CO_2 \quad (25)$$

In comparison to the discharge without a catalyst, the presence of the Ni catalysts in the DBD increases the amplitude and number of current pulses in the current signals (Figure 6). A similar phenomenon has also been reported in the previous study.[8] The combination of

plasma and the Ni/γ-Al_2O_3 catalyst gave the highest CO_2 conversion of 26.2% and CH_4 conversion of 44.1% at a SED of 72 kJ l^{-1}. The catalyst activity for biogas conversion follows the order: Ni/γ-Al_2O_3 > Ni/MgO > Ni/SiO_2 > Ni/TiO_2. Compared to the plasma reforming without a catalyst, the integration of plasma with the Ni/γ-Al_2O_3 catalyst enhances the conversion of CO_2 and CH_4 by 10.1% and 5.7 %, respectively.

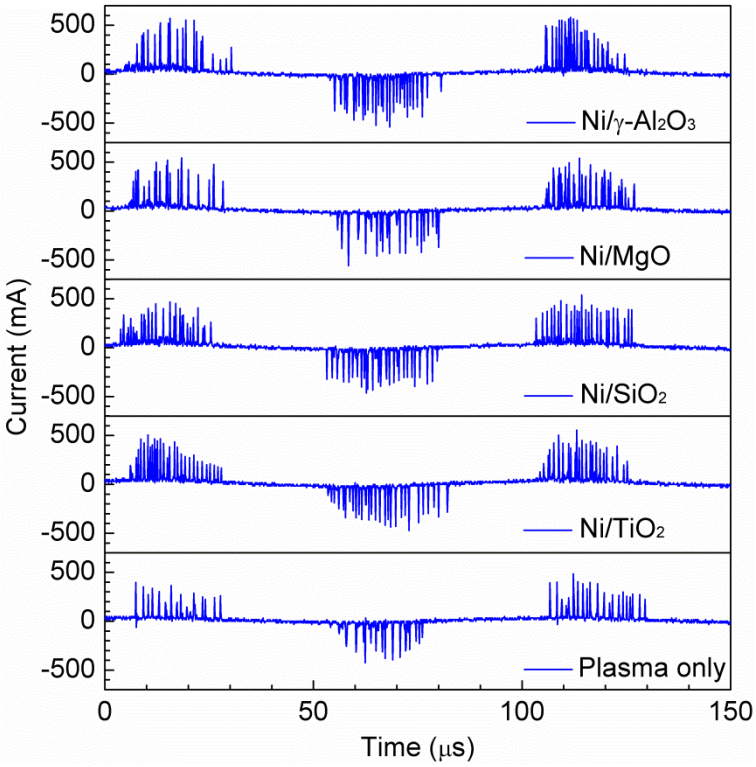

Figure 6. Current signals of CO_2/CH_4 DBD, with and without a catalyst (SED = 60 kJ l^{-1}; total feed flow rate: 50 ml min^{-1}; CO_2/CH_4 molar ratio: 1:1).

Generally, catalysts with higher specific surface area could provide larger contact area and more active sites for surface reactions to occur, resulting in higher reaction activity.[40, 41] The smaller metal particle size on the catalyst surface also plays an important role in reducing coke deposition on the catalysts and enhancing the reaction performance.[41, 42] Compared with other Ni catalysts in this work, larger specific surface area and smaller NiO crystalline size of the Ni/γ-Al_2O_3 catalyst contribute to higher catalytic performance in the plasma

reforming process. In this process, CO_2 reactant molecules can be dissociated to CO while releasing O atoms, which can enhance the dissociation of CH_4 and reduce carbon formation on the catalyst.[43] The catalysts with a greater number of strong basic sites can enhance the adsorption of CO_2 onto the catalyst surface and hence supply more oxygen species for the gasification of intermediate carbonaceous species from CH_4 decomposition, which consequently leads to a reduction in carbon deposition on the catalyst surface.[40] Therefore, the increased presence of strong basic sites on the Ni/γ-Al_2O_3 catalyst might be another reason for the higher conversion of CO_2 and CH_4, compared with the conversions obtained when using other catalysts.

In thermal catalytic dry reforming of CH_4, high temperatures (> 700 ^oC) are required to activate Ni-based catalysts.[30] The combination of non-thermal plasma and catalyst can lower the activation barrier of Ni catalysts. In this study, the maximum temperature inside the plasma-catalytic reactor is lower than 230 ^oC under our experimental conditions. Our previous thermodynamic equilibrium calculation of dry reforming of CH_4 confirmed that the conversion of CO_2 and CH_4 was very low (<1%) at low temperatures (e.g. 300 ^oC),[8] which suggests that extremely low CO_2 and CH_4 conversions can be obtained in the thermal catalytic dry reforming reaction below 300 ^oC. These results show a synergistic effect when combining plasma and different Ni catalysts at low temperatures.

3.2.2 Production of syngas and C_2-C_4 hydrocarbons

Figure 7 shows the effect that different Ni catalysts have on the production of syngas. Clearly, under all the experimental conditions, the yield of CO and H_2 is increased by increasing the SED. At a specified SED, packing the Ni catalysts into the DBD reactor enhances the yield of CO and H_2. The highest yield of CO (16.8%) and H_2 (15%) is achieved at a SED of 72 kJ l^{-1} when the Ni/γ-Al_2O_3 catalyst is combined with the plasma, followed by the Ni/MgO, Ni/SiO_2 and Ni/TiO_2 catalysts, which is in accordance with their activity for the

conversions of CO_2 and CH_4. Compared with the plasma reforming of biogas without a catalyst, placing the Ni/γ-Al_2O_3 catalyst in the DBD enhances the yield of CO and H_2 by 9.9% and 15.9%, respectively.

The combination of plasma and Ni catalysts also increases the selectivity to CO and H_2. This effect differs from previous results reported by Song et al.[44] They found that the presence of a Ni/Al_2O_3 catalyst in a DBD reactor slightly decreased the selectivity of H_2 but increased the selectivity of CO in the plasma-catalytic dry reforming of methane, compared to plasma reforming with no catalyst. In this study, the effect of the catalysts on the selectivity to CO and H_2, from low to high, follows the order of Ni/TiO_2 < Ni/SiO_2 < Ni/MgO < Ni/γ-Al_2O_3, which is in accordance with their effect on the yield of CO and H_2 at a specified SED. The highest selectivity to CO and H_2 is 48.8 % and 34.6%, respectively, when the Ni/γ-Al_2O_3 catalyst is used at a SED of 36 kJ l^{-1}. Increasing the SED decreases the selectivity of CO and H_2, regardless of the catalysts used. This phenomenon might be ascribed to the formation of carbon deposition or of higher hydrocarbons by increasing the SED. Jiang et al also reported similar evolution in the selectivity to CO and H_2 as a function of SED.[45] They found that the selectivity to CO and H_2 decreased from 50.8% and 52.2% to 42.8% and 23.2%, respectively, when increasing the input power from 100 to 500 W in a plasma-catalytic dry reforming reaction over a zeolite A catalyst at a total feed flow rate of 200 ml min^{-1} with a CO_2/CH_4 molar ratio of 1:1.[45]

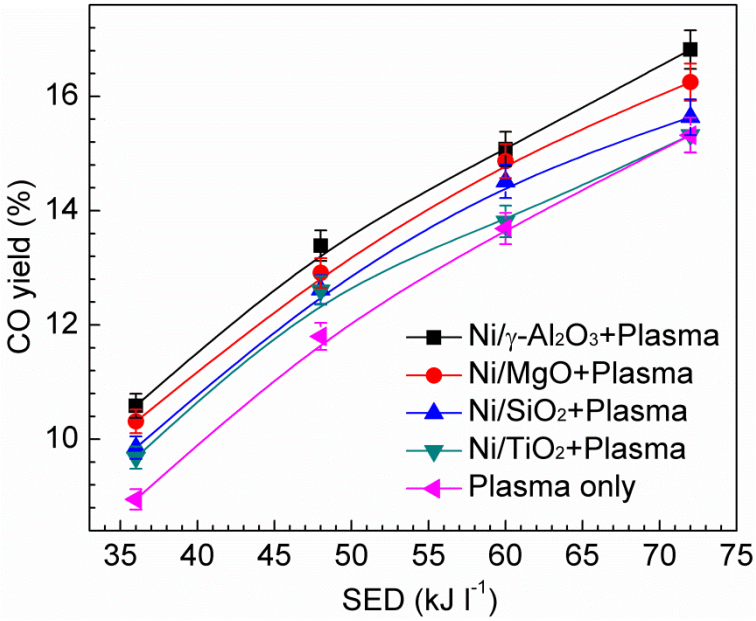

410

411 (a)

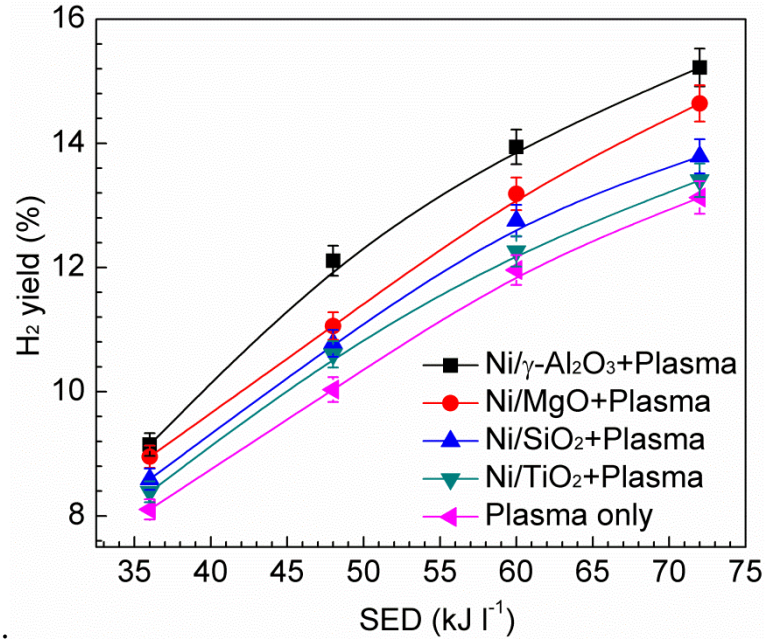

412 .

413 (b)

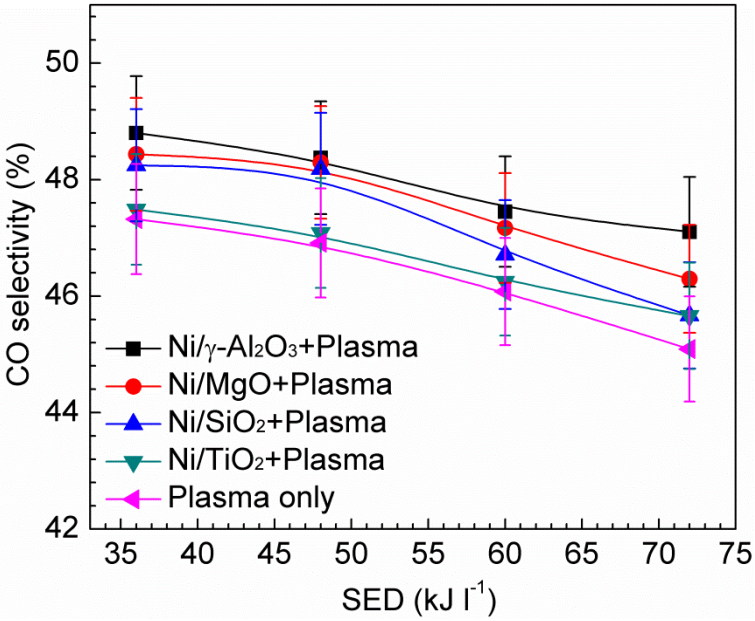

(c)

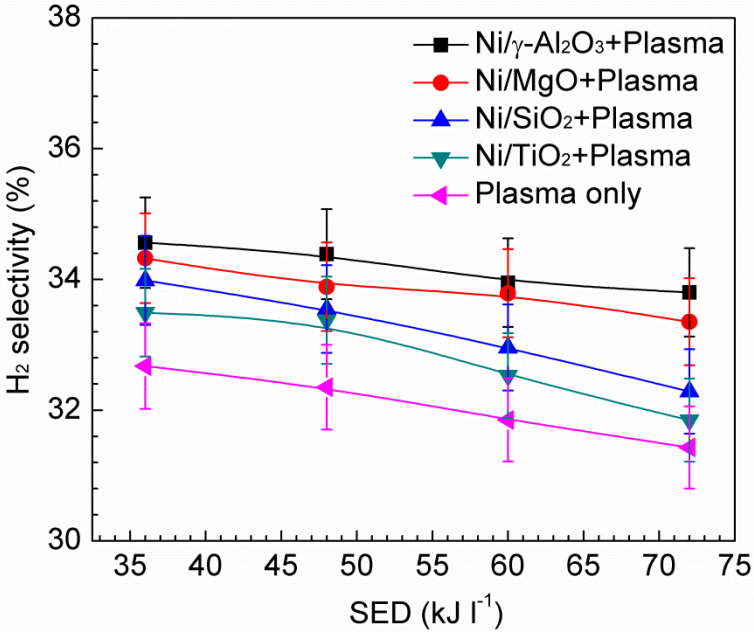

(d)

Figure 7. Effect of different Ni catalysts on the syngas production as a function of SED: (a) CO yield; (b) CO selectivity; (c) H_2 yield; (d) H_2 selectivity (total feed flow rate: 50 ml min^{-1}; CO_2/CH_4 molar ratio: 1:1).

Figure 8 shows the influence of Ni catalysts with different supports on the selectivity of C_2-C_4 hydrocarbons. In our experiments, the main C_2-C_4 hydrocarbons were C_2H_6, C_3H_8 and

C_4H_{10}, while only a trace amount of C_2H_2 and C_2H_4 were formed. The selectivity towards C_3H_8 and C_4H_{10} shows an increase when increasing the SED. In contrast, increasing the SED decreases the selectivity to C_2H_6. Previous simulation has shown that the reaction (Equation 20) is responsible for 79% of the total electron impact dissociation of CH_4,[46, 47] which generates CH_3 as the main radical. C_2H_6 is mainly formed from the recombination of CH_3 radicals through the neutral-neutral reaction (Equation 26). Meanwhile, C_2H_6 can be consumed by the reaction with CH_3 radicals (Equation 27) or by electron impact dissociation to form C_2H_4 or C_2H_5 (Equation 28 and 29).[39, 48, 49] The produced radicals favour the formation of other hydrocarbons, such as C_3H_8 and C_4H_{10}, from the neutral-neutral reactions (Equation 30 and 31). This suggests that increasing the SED results in the decomposition of C_2H_6 to form other hydrocarbons, confirmed by the slight increase in the selectivity to C_3H_8 and C_4H_{10}.

$$CH_3 + CH_3 \rightarrow C_2H_6 \quad (26)$$

$$CH_3 + C_2H_6 \rightarrow C_2H_5 + CH_4 \quad (27)$$

$$e + C_2H_6 \rightarrow e + C_2H_5 + H \quad (28)$$

$$e + C_2H_6 \rightarrow e + C_2H_4 + H_2 \quad (29)$$

$$C_2H_5 + CH_3 \rightarrow C_3H_8 \quad (30)$$

$$C_2H_5 + C_2H_5 \rightarrow C_4H_{10} \quad (31)$$

The highest selectivity towards C_3H_8 (5.6 %) and C_4H_{10} (4.4 %) is achieved when the Ni/γ-Al_2O_3 catalyst is placed in the DBD at a SED of 72 kJ l^{-1}. In contrast, the presence of the Ni catalysts in the plasma biogas reforming decreases the selectivity to C_2H_6. The maximum C_2H_6 selectivity of 22.2% is obtained in the plasma reforming without a catalyst at a SED of 36 kJ l^{-1}.

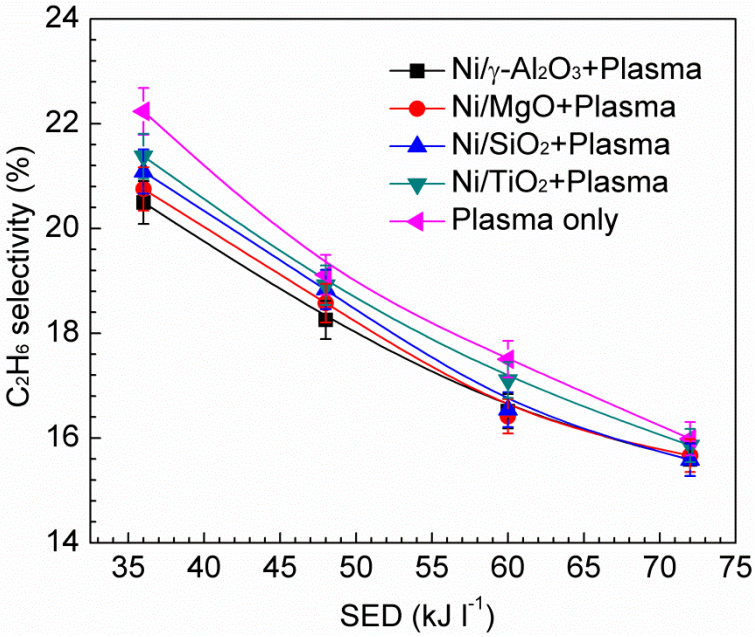

447

448 (a)

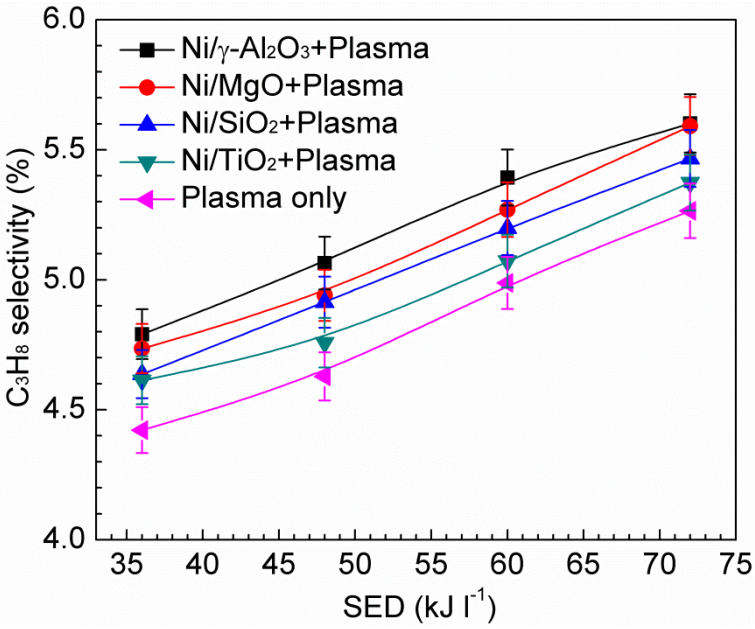

449

450 (b)

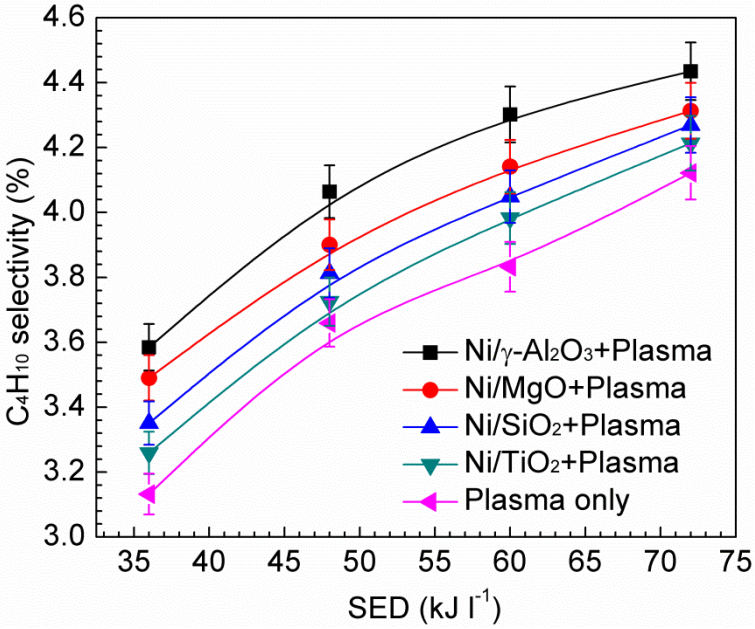

(c)

Figure 8. Effect of different catalysts on the selectivity to C_2-C_4 hydrocarbons (a) C_2H_6; (b) C_3H_8; (c) C_4H_{10} (total feed flow rate: 50 ml min^{-1}; CO_2/CH_4 molar ratio: 1:1).

3.2.3 Carbon balance

Figure 9 shows the carbon balance of the plasma-catalytic biogas reforming using different Ni catalysts as a function of SED. At a SED of 36 kJ l^{-1}, the carbon balance is over 95% regardless of the catalyst used. Note that increasing the SED decreases the carbon balance in the plasma reforming of biogas. This might be due to an increase in carbon deposition or to the formation of higher hydrocarbons (e.g. C_{5+}) and liquid oxygenates.[50] Compared to the plasma reforming reaction without a catalyst, the combination of plasma and these Ni catalysts slightly increases the carbon balance, with the exception of the Ni/TiO_2 catalyst. The plasma-catalytic reforming process that uses the Ni/γ-Al_2O_3 catalyst shows the highest carbon balance (96.4%) at a SED of 36 kJ l^{-1}. This is followed, in decreasing order, by that obtained when using the Ni/MgO, Ni/SiO_2 and Ni/TiO_2 catalysts.

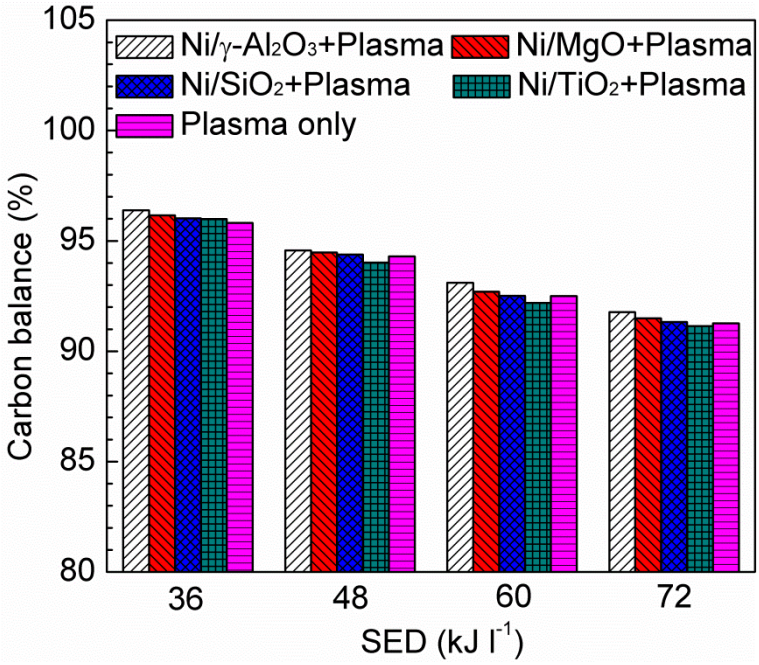

468

469 *Figure 9.* Effect of different Ni catalysts on the carbon balance of the plasma-catalytic dry
470 reforming process as a function of SED (total feed flow rate: 50 ml min^{-1}; CO_2/CH_4 molar
471 ratio: 1:1).

472

473 Figure 10 shows the TG results of the spent Ni catalysts after the plasma-catalytic reaction
474 had been running for 150 min. The spent Ni/γ-Al_2O_3 catalyst shows the lowest carbon
475 deposition of 3.8%, followed by the spent Ni/MgO (4.2%), Ni/SiO_2 (4.9%) and Ni/TiO_2
476 (5.3%) catalysts. This might be ascribed to the increased formation of strong basic sites on the
477 Ni/γ-Al_2O_3 catalyst (Figure 3). The carbon deposition on these Ni catalysts is not only lower
478 than that used in thermal catalytic biogas reforming,[51-53] but also lower than the carbon
479 deposition reported in previous plasma-catalytic dry reforming processes.[16, 54] For instance,
480 Wang et al reported that the carbon deposition was 5.4% and 11.5% when using reduced and
481 unreduced Ni/γ-Al_2O_3 catalysts in the plasma-catalytic dry reforming of CH_4 in a DBD
482 reactor.[54]

483

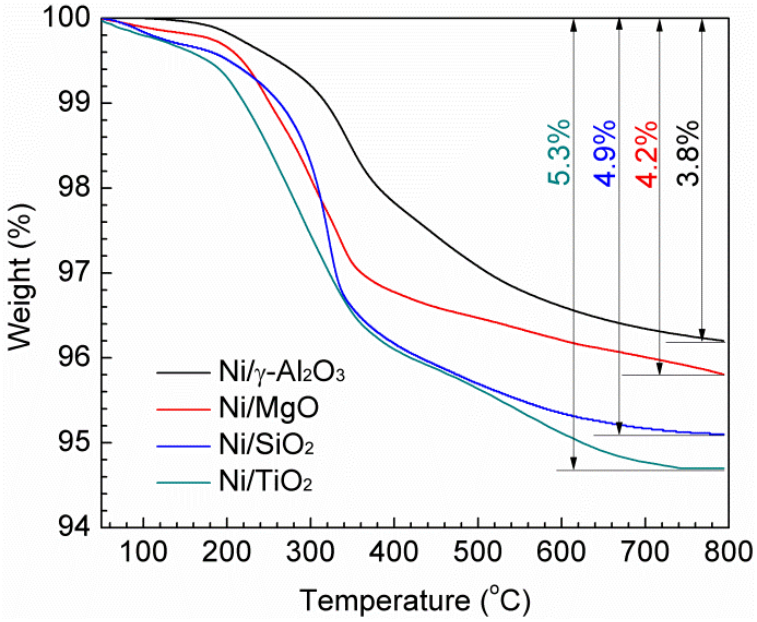

Figure 10. TG results of different Ni catalysts after reaction at a SED of 60 kJ l^{-1} for 150 min.

3.2.4 Energy performance of the plasma-catalytic process

Figure 11 shows the effect that different supported Ni catalysts have on the energy cost, energy efficiency and fuel production efficiency of the plasma biogas reforming process at a SED of 36 kJ l^{-1}. The energy cost for CO_2 conversion is higher than that for CH_4 conversion in the plasma reforming process both with and without a catalyst. The presence of the Ni catalysts in the plasma reduces the energy cost for biogas conversion. When the Ni/γ-Al_2O_3 catalyst is used, the lowest energy cost for CO_2 conversion, CH_4 conversion and total carbon conversion is 9.9 MJ mol^{-1}, 6.2 MJ mol^{-1} and 3.8 MJ mol^{-1}, respectively, 5-7.5% lower in comparison to the plasma biogas reforming without a catalyst. Similarly, the Ni/γ-Al_2O_3 catalyst also shows the lowest energy cost for syngas production. The combination of plasma with the Ni catalysts also enhances the energy efficiency and fuel production efficiency of the plasma reforming of biogas. The highest energy efficiency (0.263 mmol kJ^{-1}) and fuel production efficiency (10.4%) are achieved when the Ni/γ-Al_2O_3 catalyst is partially packed into the DBD reactor. Both values are higher than those obtained for the plasma biogas reforming without a catalyst.

502

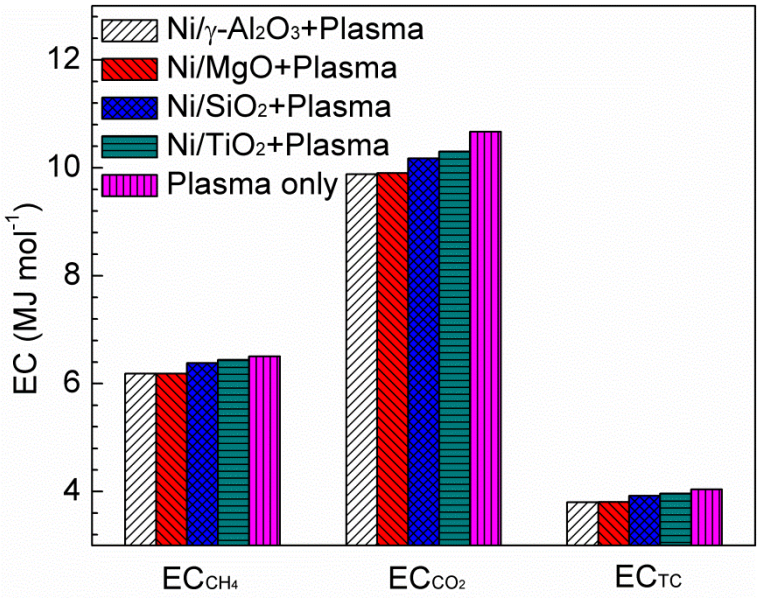

503

504 (a)

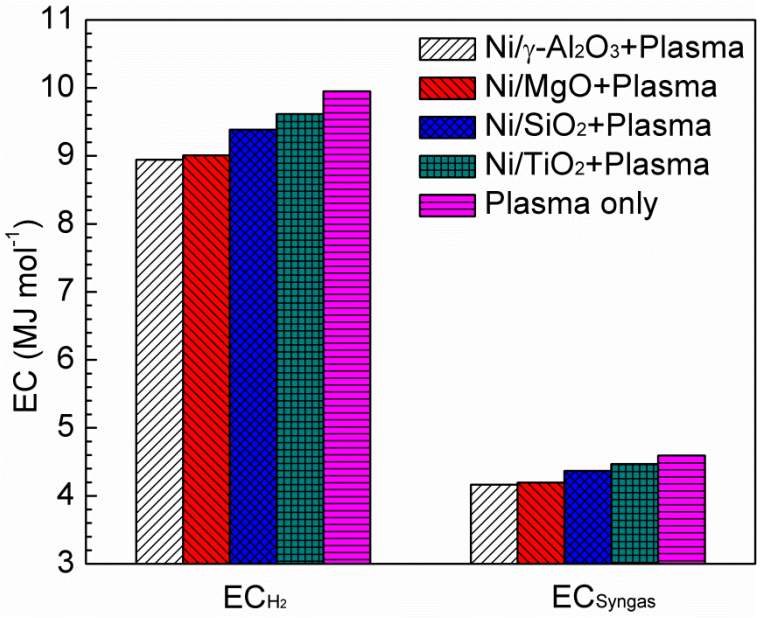

505

506 (b)

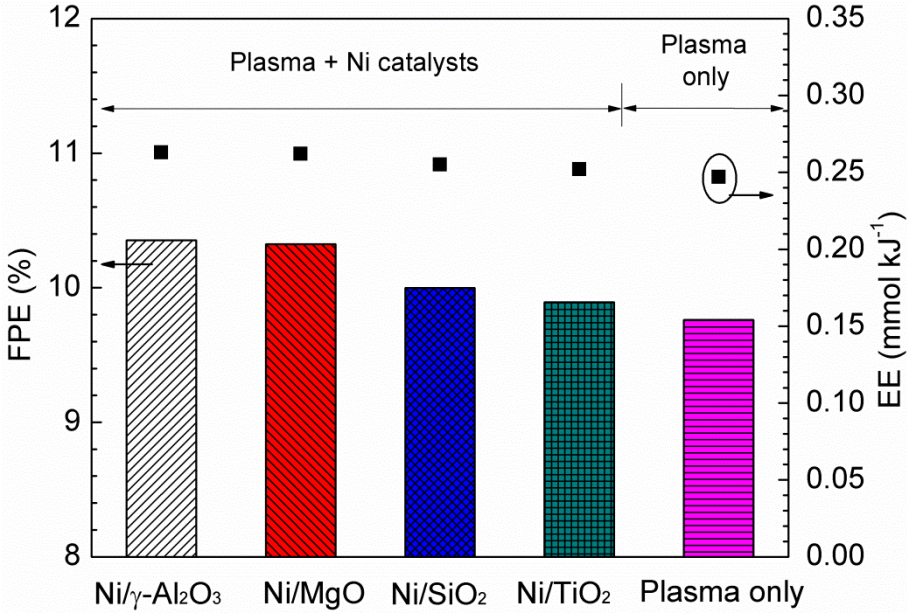

(c)

Figure 11. Effect of different catalysts on (a) the energy cost for CH_4 conversion, CO_2 conversion and total carbon conversion; (b) the energy cost H_2 and syngas production; (c) the energy efficiency and fuel production efficiency (SED: 36 kJ l^{-1}; total feed flow rate: 50 ml min^{-1}; CO_2/CH_4 molar ratio: 1:1).

Table 3 shows a comparison of the fuel production efficiency of plasma dry reforming of CH_4 using different catalysts. DBD reactors have been the most commonly used in the plasma-catalytic reforming of methane as catalysts can be easily integrated with a DBD reactor, either using a single-stage or a two-stage configuration. DBD systems can be scaled up by integrating a number of coaxial tubular reactors to increase treatment capacity of the system for industrial scale applications. This has been successfully demonstrated in large scale water treatment, gas cleaning and ozone generation.[10, 55, 56] Therefore, only plasma-catalytic dry reforming reactions using DBD plasmas have been included in Table 2. Clearly, higher discharge power results in higher conversions of CO_2 and CH_4, but lowers the fuel production efficiency of the plasma-catalytic process. Higher feed flow rate leads to higher fuel production efficiency but significantly decreases the conversion of reactants. This trade-

off between the discharge power and feed flow rate has also been reported in previous studies,[35, 57] which suggests that further optimization of the plasma-catalytic system (including reactor geometry, power supply, operating parameters and catalysts) is required to overcome this issue. For example, using pulsed power might provide a promising way to enhance the energy efficiency of the plasma process at a relatively low power and high flow rate. The combination of the plasma process with a gas separation process might also provide a solution by recycling unreacted input gases, which could enhance the overall energy efficiency of the plasma process through a chemical looping process.

In this study, the maximum fuel production efficiency of 10.4% is achieved when the Ni/γ-Al_2O_3 catalyst is combined with the plasma (without extra heating) at a discharge power of 30 W and a total feed flow rate of 50 ml min^{-1}. This value is comparable to the results obtained in previous works using similar DBDs (Table 3). Zhang et al reported that using a Ni-Cu bimetallic catalyst (12 wt.%Ni-12 wt.% Cu/γ-Al_2O_3) in the plasma-catalytic dry reforming of CH_4 showed higher conversions of the reactants (CO_2: 75.3%; CH_4: 69.8%), and greater product selectivity (H_2: 56.6%; CO: 76.0%) compared with 12 wt.% Ni/γ-Al_2O_3 and 12 wt.% Cu/γ-Al_2O_3 catalysts.[20] However, this experiment was carried out using Ar as the carrier gas with an extra thermal heating of 450 ^oC. If the energy for heating is considered, the FPE of this process will be much lower than the value presented in Table 2. In addition, the synergy between the Ni and Cu species in the Ni-Cu bimetallic catalyst has not been satisfactorily explained.[20] Zheng et al prepared a core-shell structured $LaNiO_3$@SiO_2 nano-particle catalyst for plasma dry reforming of methane and obtained a high total carbon conversion of 83.0% with a H_2 selectivity of 83.7% and a CO selectivity of 92.4%.[24] This reaction was performed at a high discharge power of 150 W, which lowered the fuel production efficiency to 7.3%.[24] Goujard et al used a mono-polar pulsed DBD reactor for biogas reforming over a perovskite $LaNiO_3$ catalyst at a low discharge power (25 W) but with external heating to 600 ^oC.[23] The estimated FPE of this process was 8.5 % which could be much lower if we

consider the energy from thermal heating. It was difficult to understand whether the catalyst was activated by the plasma and/or high temperature heating. Therefore, further optimization of the plasma-catalytic process for biogas reforming should focus on the development of new catalysts which are highly active, even at low energy inputs and temperatures, and have high stability in order to maximize the performance of the plasma-catalytic reforming process and make it economically feasible.

Table 3. Comparison of the FPE in different plasma-catalytic reforming processes

Plasma reactor	Discharge power (W)	Total feed flow rate (ml min^{-1})	CO_2/CH_4 molar ratio	Catalyst	Conversion (%)			Selectivity (%)		EC_{H2} (MJ mol^{-1})	FPE (%)	Ref
					CH_4	CO_2	Total	H_2	CO			
DBD	30	50	1:1	10 wt.% Ni/ γ-Al_2O_3	26.1	16.3	21.2	34.6	48.8	8.9	10.4	This study
DBD	500	800	1:1	Zeolite NaX	20.1	15.3	17.7	-	40.1	-	6.4	[12]
DBD	500	600	1:1	Zeolite NaY	34.7	15.2	25.0	23.2	45.0	13.9	9.3	[13]
DBD	500	200	1:3	Zeolite A	54.8	25.3	47.4	48.1	26.8	8.5	8.6	[45]
DBD	130	30	1:1	7 wt.% Ni/ γ-Al_2O_3	55.5	32.6	44.0	53.5	63.9	19.6	3.2	[44]
DBD	50	50	1:1	10 wt.%Ni/ γ-Al_2O_3	56.4	30.2	43.3	31.0	52.4	7.7	16.4	[8]
DBD	60	30	1:1	12 wt.%Ni-12 wt.% Cu/γ-Al_2O_3	69.8	75.3	72.6	56.6	76.0	6.8	8.5	[20]
DBD	150	40	1:1	$LaNiO_3$@SiO_2	88.3	77.8	83.0	83.7	92.4	6.8	7.3	[24]
Pulsed DBD	25	22.5	3:2	Perovskite $LaNiO_3$	54.5	73.0	61.9	38.2	50.4	6.0	8.5	[23]

4. Conclusions

In this study, the plasma-catalytic dry reforming of simulated biogas over different supported Ni catalysts (Ni/γ-Al_2O_3, Ni/MgO, Ni/SiO_2 and Ni/TiO_2) has been performed in a coaxial DBD reactor. The performance of the plasma-catalytic dry reforming process is enhanced by combining the supported Ni catalysts with DBD plasma. The maximum CO_2

conversion of 26.2% and CH_4 conversion of 44.1% are achieved when the Ni/γ-Al_2O_3 catalyst is introduced into the DBD reactor at a SED of 72 kJ l^{-1}. The highest production of syngas and C_3-C_4 hydrocarbons, but the lowest production of C_2 hydrocarbon, is observed when the Ni/γ-Al_2O_3 catalyst is used at a specified specific energy density. Combining the Ni/γ-Al_2O_3 catalyst with plasma also leads to the lowest energy cost for reactant conversions and syngas production, as well as the maximum energy efficiency and fuel production efficiency. After the plasma-catalytic reaction has been running for 150 min at a SED of 60 kJ l^{-1}, the carbon deposition on the spent Ni/γ-Al_2O_3 catalyst is only 3.8%, which is lower than the conventional thermal catalytic and previous plasma-catalytic dry reforming processes using similar Ni-based catalysts. Compared to other catalysts, the enhanced plasma catalytic activity of the Ni/γ-Al_2O_3 catalyst can be ascribed to its higher specific surface area, higher dispersion and smaller particle size of NiO, greater number of strong basic sites and its high reducibility.

Acknowledgements: The support of this work by the EPSRC SUPERGEN Hydrogen & Fuel Cell (H2FC) Programme is gratefully acknowledged.

Received: ((will be filled in by the editorial staff)); Revised: ((will be filled in by the editorial staff)); Published online: ((please add journal code and manuscript number, e.g., DOI: 10.1002/ppap.201100001))

Keywords: Plasma-catalysis; biogas reforming; dielectric barrier discharge; Ni catalysts

References

[1] G. Urbini, M. Raboni, *Rev. Ambient. Água.* **2014**, *9*, 191.

[2] S. Liu, D.H. Mei, L. Wang, X. Tu, 2016, *Chem. Eng. J.* 2016, 10.1016/j.cej.2016.08.005

[3] L. Wang, S. Liu, C. Xu, X. Tu, 2016, *Green Chem.* 2016, 10.1039/C6GC01604A

[4] J. C. Whitehead, *J. Phys. D: Appl. Phys.* **2016**, *49*, 243001.

[5] E. C. Neyts, K. Ostrikov, M. K. Sunkara, A. Bogaerts, *Chem. Rev.* **2015**, *115*, 13408.

[6] D.H. Mei, X. Zhu, C. Wu, B. Ashford, P. T. Williams, X. Tu, *Appl. Catal. B-Environ.* **2016**, *182*, 525.

[7] D.H. Mei, X. B. Zhu, Y. L. He, J. D. Yan, X. Tu, *Plasma Sources Sci. Technol.* **2015**, *24*, 015011.

[8] X. Tu, J. C. Whitehead, *Appl. Catal. B-Environ.* **2012**, *125*, 439.

[9] R. Aerts, X. Tu, W. Van Gaens, J. C. Whitehead, A. Bogaerts, *Environ. Sci. Technol.* **2013**, *47*, 6478.

[10] A. Mizuno, *Catal. Today* **2013**, *211*, 2.

[11] H. J. Gallon, X. Tu, J. C. Whitehead, *Plasma Process. Polym.* **2012**, *9*, 90.

[12] B. Eliasson, C. J. Liu, U. Kogelschatz, *Ind. Eng. Chem. Res.* **2000**, *39*, 1221.

[13] K. Zhang, U. Kogelschatz, B. Eliasson, *Energ. Fuel.* **2001**, *15*, 395.

[14] S. Mahammadunnisa, P. M. K. Reddy, B. Ramaraju, C. Subrahmanyam, *Energ. Fuel.* **2013**, *27*, 4441.

[15] X. Tu, H. J. Gallon, M. V. Twigg, P. A. Gorry, J. C. Whitehead, *J. Phys. D: Appl. Phys.* **2011**, *44*, 274007.

[16] Q. Wang, Y. Cheng, Y. Jin, *Catal. Today* **2009**, *148*, 275.

[17] Y. X. Zeng, X. B. Zhu, D. H. Mei, B. Ashford, X. Tu, *Catal. Today* **2015**, *256*, 80.

[18] J. Sentek, K. Krawczyk, M. Mlotek, M. Kalczewska, T. Kroker, T. Kolb, A. Schenk, K.-H. Gericke, K. Schmidt-Szalowski, *Appl. Catal. B-Environ.* **2010**, *94*, 19.

[19] T. Kroker, T. Kolb, A. Schenk, K. Krawczyk, M. Mlotek, K. H. Gericke, *Plasma Chem. Plasma Process.* **2012**, *32*, 565.

[20] A.-J. Zhang, A.-M. Zhu, J. Guo, Y. Xu, C. Shi, *Chem. Eng. J.* **2010**, *156*, 601.

[21] K. Krawczyk, M. Mlotek, B. Ulejczyk, K. Schmidt-Szalowski, *Fuel* **2014**, *117*, 608.

[22] M. H. Pham, V. Goujard, J. M. Tatibouet, C. Batiot-Dupeyrat, *Catal. Today* **2011**, *171*, 67.

[23] V. Goujard, J. M. Tatibouet, C. Batiot-Dupeyrat, *Appl. Catal. A-Gen.* **2009**, *353*, 228.

[24] X. Zheng, S. Tan, L. Dong, S. Li, H. Chen, *Int. J. Hydrogen Energy* **2014**, *39*, 11360.

[25] X. G. Zheng, S. Y. Tan, L. C. Dong, S. B. Li, H. M. Chen, *Chem. Eng. J.* **2015**, *265*, 147.

[26] M. Usman, W. M. A. W. Daud, H. F. Abbas, *Renew. Sust. Energ. Rev.* **2015**, *45*, 710.

[27] J. Gao, Z. Hou, H. Lou, X. Zheng, in *Fuel Cells: Technologies for Fuel Processing* (Eds: D. Shekhawat, J.J. Spivey, D.A. Berry), Elsevier, Oxford, UK **2011,** Ch. 7.

[28] Heat of combustion, https://en.wikipedia.org/wiki/Heat_of_combustion.

[29] J. Feng, Y. Ding, Y. Guo, X. Li, W. Li, *Fuel Processing Technology* **2013**, *109*, 110.

[30] Y.-H. Wang, H.-M. Liu, B.-Q. Xu, *J. Mol. Catal. A: Chem.* **2009**, *299*, 44.

[31] X. Tu, H. J. Gallon, J. C. Whitehead, *Catal. Today* **2013**, *211*, 120.

[32] L. Pino, A. Vita, F. Cipiti, M. Lagana, V. Recupero, *Appl. Catal. B-Environ.* **2011**, *104*, 64.

[33] S. B. Wang, G. Q. M. Lu, *J. Chem. Technol. Biotechnol.* **2000**, *75*, 589.

[34] T. Horiuchi, K. Sakuma, T. Fukui, Y. Kubo, T. Osaki, T. Mori, *Appl. Catal. A-Gen.* **1996**, *144*, 111.

[35] X. Yang, Y. Wang, M. Li, B. Sun, Y. Li, Y. Wang, *Energ. Fuel.* **2016**, *30*, 2198.

[36] A. Ozkan, T. Dufour, T. Silva, N. Britun, R. Snyders, A. Bogaerts, F. Reniers, *Plasma Sources Sci. Technol.* **2016**, *25*, 025013.

[37] D.H. Mei, Y.-L. He, S. Liu, J. Yan, X. Tu, *Plasma Process. Polym.* **2016**, *13*, 544.

[38] L. M. Zhou, B. Xue, U. Kogelschatz, B. Eliasson, *Energ. Fuel.* **1998**, *12*, 1191.

[39] R. Snoeckx, R. Aerts, X. Tu, A. Bogaerts, *J. Phys. Chem. C* **2013**, *117*, 4957.

[40] M. A. Naeem, A. S. Al-Fatesh, A. E. Abasaeed, A. H. Fakeeha, *Fuel Process. Technol* **2014**, *122*, 141.

643 [41] Q. Zhang, T. Wu, P. Zhang, R. J. Qi, R. Huang, X. F. Song, L. Gao, *RSC Adv.* **2014**,
644 *4*, 51184.
645 [42] X. B. Zhu, X. Gao, R. Qin, Y. X. Zeng, R. Y. Qu, C. H. Zheng, X. Tu, *Appl. Catal.*
646 *B-Environ.* **2015**, *170*, 293.
647 [43] D. Pakhare, J. Spivey, *Chem. Soc. Rev.* **2014**, *43*, 7813.
648 [44] H. K. Song, J. W. Choi, S. H. Yue, H. Lee, B. K. Na, *Catal. Today* **2004**, *89*, 27.
649 [45] T. Jiang, Y. Li, C. J. Liu, G. H. Xu, B. Eliasson, B. Z. Xue, *Catal. Today* **2002**, *72*,
650 229.
651 [46] C. De Bie, B. Verheyde, T. Martens, J. van Dijk, S. Paulussen, A. Bogaerts, *Plasma*
652 *Process. Polym.* **2011**, *8*, 1033.
653 [47] C. De Bie, J. van Dijk, A. Bogaerts, *J. Phys. Chem. C* **2015**, *119*, 22331.
654 [48] Y. Yang, *Ind. Eng. Chem. Res.* **2002**, *41*, 5918.
655 [49] R. K. Janev, D. Reiter, *Phys. Plasmas* **2004**, *11*, 780.
656 [50] M.-W. Li, Y.-L. Tian, G.-H. Xu, *Energ. Fuel.* **2007**, *21*, 2335.
657 [51] Y. K. Han, C.-I. Ahn, J.-W. Bae, A. R. Kim, G. Y. Han, *Ind. Eng. Chem. Res.* **2013**,
658 *52*, 13288.
659 [52] K. Tao, L. Shi, Q. Ma, D. Wang, C. Zeng, C. Kong, M. Wu, L. Chen, S. Zhou, Y. Hu,
660 N. Tsubaki, *Chem. Eng. J.* **2013**, *221*, 25.
661 [53] L. M. Zhang, L. Li, Y. H. Zhang, Y. X. Zhao, J. L. Li, *J Energ. Chem.* **2014**, *23*, 66.
662 [54] Q. Wang, B.-H. Yan, Y. Jin, Y. Cheng, *Energ. Fuel.* **2009**, *23*, 4196.
663 [55] T. Nozaki, K. Okazaki, *Green Process. Synth.* **2012**, *1*, 517.
664 [56] H. L. Chen, H. M. Lee, S. H. Chen, M. B. Chang, *Ind. Eng. Chem. Res.* **2008**, *47*,
665 2122.
666 [57] R. Snoeckx, Y. X. Zeng, X. Tu, A. Bogaerts, *RSC Adv.* **2015**, *5*, 29799.
667

Table of contents

Plasma-catalytic reforming of biogas over supported Ni catalysts in a dielectric barrier discharge reactor: Effect of catalyst supports

Danhua Mei, Bryony Ashford, Ya-Ling He, Xin Tu*

Plasma-catalytic reforming of biogas over supported Ni catalysts has been investigated in a coaxial dielectric barrier discharge reactor at low temperatures. The effects of the catalyst supports have been evaluated in terms of the conversions of biogas, the yield and selectivity of target products, the carbon deposition on the spent catalysts and the energy efficiency of the plasma catalytic process.